

Dynamical entropy of the separatrix map

Ivan I. Shevchenko*

Saint Petersburg State University, 7/9 Universitetskaya nab.,
199034 Saint Petersburg, Russia

Institute of Applied Astronomy of the Russian Academy of Sciences,
191187 Saint Petersburg, Russia

Abstract

We calculate the maximum Lyapunov exponent of the motion in the separatrix map's chaotic layer, along with calculation of its width, as functions of the adiabaticity parameter λ . The separatrix map is set in natural variables; and the case of the layer's least perturbed border is considered, i. e., the winding number of the layer's border (the last invariant curve) is the golden mean. Although these two dependences (for the Lyapunov exponent and the layer width) are strongly non-monotonous and evade any simple analytical description, the calculated dynamical entropy h turns out to be a close-to-linear function of λ . In other words, if normalized by λ , the entropy is a quasi-constant. We discuss whether the function $h(\lambda)$ can be in fact exactly linear, $h \propto \lambda$. The function $h(\lambda)$ forms a basis for calculating the dynamical entropy for any perturbed nonlinear resonance in the first fundamental model, as soon as the corresponding Melnikov–Arnold integral is estimated.

*E-mail: ivan.i.shevchenko@gmail.com

1 Introduction

In [8, p. 37], Boris Chirikov, when considering the Krylov–Kolmogorov (dynamical) entropy, notes that the term entropy here “cannot be regarded as felicitous, because there is confusion with the usual thermodynamic entropy. In fact these quantities are completely different even in dimension.” Then, by introducing a minimum permissible volume of phase space, defined as the correlation volume (inside which the motion is not chaotic), Chirikov arrives to a dynamical characterization of entropy of a chaotic system. Indeed, the correlation volume exponentially decreases with time, opposite to the usual definition case for the minimum volume, when the latter is determined by the phase space quantization and is constant in time. Then, “defined, in such a way, the dynamical entropy permanently increases with time (in a state of statistical equilibrium!) for any system with mixing” [8, p. 38]. The following formula for the dynamical entropy naturally arises:

$$h = \lim_{t \rightarrow \infty} \left(-\frac{1}{t} \int \ln \Delta \mu_c(t) d\mu \right), \quad (1)$$

where μ is the phase space measure, $\mu_c(t)$ is the correlation volume as a function of time t , and the integration is performed over the whole chaotic domain where the motion takes place; see [8, eq. (2.3.14)]. The dynamical entropy h has dimension of frequency. In [8, 6], it is called K-entropy (Kolmogorov entropy); and, in [11], KS-entropy (Kolmogorov–Sinai entropy).

On assuming that the local Lyapunov exponent value is constant over the chaotic domain, formula (1) is straightforwardly reducible to an approximate one, on other grounds proposed in [6, eq. (6)]:

$$h = L\mu_{\text{ch}}, \quad (2)$$

where L is the maximum Lyapunov exponent in the chaotic domain, and μ_{ch} is the latter’s measure.

On variations of any parameter of a system under study, appearance/disappearance of regular islands (including those due to marginal resonances) in the phase space often induce disturbances in the dependences of L and μ_{ch} on the parameter. However, in the dependence of the product $L\mu_{\text{ch}}$ on the given parameter these disturbances are usually observed to compensate each other, so that the resulting dependence is smooth; spectacular examples can be found in [24, figs. 1–4] for the standard map case; and, for the separatrix

map, in [28, figs. 1b, 1c]. This smoothing-out effect graphically demonstrates, as nothing else, the fundamental character of the dynamical entropy.

Generally, the separatrix maps describe the motion in the vicinity of the separatrices of nonlinear resonances subject to periodic perturbations. Construction and analysis of separatrix maps constitute a powerful tool of modern nonlinear dynamics [11, 5, 3, 4, 31, 32, 27, 22, 1, 2, 30].

Under general conditions [11, 18], a model of a nonlinear resonance is provided by the nonlinear pendulum with periodic perturbations. This is the so-called first fundamental model of perturbed nonlinear resonance, see a review in [26]. Its Hamiltonian is given by

$$H = \frac{\mathcal{G}p^2}{2} - \mathcal{F} \cos \varphi + a (\cos(k\varphi - \tau) + \cos(k\varphi + \tau)), \quad (3)$$

where $\tau = \Omega t + \tau_0$. The first two terms in Eq. (3) represent the Hamiltonian H_0 of the unperturbed pendulum, while the two remaining ones the periodic perturbations. The variable φ is the resonance phase; τ is the phase angle of perturbation; Ω is the perturbation frequency, and τ_0 is the initial phase of the perturbation; p is the momentum; \mathcal{F} , \mathcal{G} , a , and integer or half-integer k are constant parameters.

A number of problems on non-linear resonances in mechanics and physics is described by the perturbed pendulum-like Hamiltonian (3). The case of symmetric perturbation $a = b$ with $k = 1$ is of especial interest. In this case, the Hamiltonian (3) describes, in particular, the pendulum with the vertically oscillating point of suspension. The near-separatrix motion of system (3) in this case was demonstrated in [11, 22] to be effectively described by the classical separatrix map.

Models with arbitrary non-zero values of integer k and zero either a or b concern the problem of a particle motion in the field of two planar waves [14, 13, 35]. In celestial mechanics, models with $k = 1/2$ and specific a and b values were applied to describe dynamics in vicinities of the 3/1 orbital resonance in planetary satellite systems [19, 30]. A model with $k = 1$ and $b = -a/7$ describes rotational dynamics close to synchronous spin-orbit resonance, of non-spherical satellites in elliptic orbits [34, 7]. By introducing *separatrix algorithmic maps* [27, 30], the separatrix map theory can be applied to a broad spectrum of physical phenomena (including the just mentioned ones), described by Hamiltonian (3).

Quantized versions of separatrix maps are broadly used in studies of quantum chaos, see [21] and references therein.

Therefore, the employed model relates with particularly interesting physical phenomena (such as the pendulum with the vibrating suspension point) and is both applicable to a broad spectrum of physical phenomena.

However, little is known nowadays on the Lyapunov exponents and the dynamical entropy of the separatrix maps, including its classical version. To elucidate the properties of the dynamical entropy of the classical separatrix map is the major goal of the present study.

We calculate the maximum Lyapunov exponent of the motion in the separatrix map's chaotic layer, along with calculation of its width, as functions of the adiabaticity parameter. The adiabaticity parameter λ is defined as the ratio of the perturbation frequency Ω to the frequency ω_0 of small-amplitude oscillations on resonance [11, 22].¹

We derive a simple approximate formula for the dynamical entropy. This might be useful in many applied problems. Indeed, computations of the Lyapunov exponents and, especially, measure of chaotic domains often represent complicated numerical tasks. Therefore, as soon as a formula connecting these two quantities is obtained, any computation of the first one automatically provides the value of the second one, and vice versa. This is especially useful for estimations of chaotic domains' measure, which is often much more complicated to obtain in numerical experiments, in comparison with Lyapunov exponents. What is more, this may provide insights for theoretical studies, which could provide analytical explanations for the observed relationships.

2 Separatrix map

Chirikov [11] derived the separatrix map that describes the motion in the vicinity of the separatrices of Hamiltonian (3) with $k = 1$:

$$\begin{aligned} w' &= w - W \sin \tau, \\ \tau' &= \tau + \lambda \ln \frac{32}{|w'|} \pmod{2\pi}, \end{aligned} \tag{4}$$

where w denotes the relative (with respect to the non-perturbed separatrix value) pendulum energy $w = \frac{H_0}{\mathcal{F}} - 1$, and τ retains its meaning of the phase

¹The *adiabaticity parameter* λ should not be confused with the *adiabatic invariant*, which is a completely different notion, whose theory is considered e.g. in [18].

angle of perturbation. The quantities λ and W are constant parameters: $\lambda = \Omega/\omega_0$, where $\omega_0 = (\mathcal{F}\mathcal{G})^{1/2}$ is frequency of small-amplitude phase oscillations (it is assumed that $\mathcal{F} > 0$, $\mathcal{G} > 0$); and

$$W = \varepsilon\lambda(A_2(\lambda) + A_2(-\lambda)) = 4\pi\varepsilon\frac{\lambda^2}{\sinh\frac{\pi\lambda}{2}}, \quad (5)$$

where $\varepsilon = a/\mathcal{F}$, and

$$A_2(\lambda) = 4\pi\lambda\frac{\exp\frac{\pi\lambda}{2}}{\sinh(\pi\lambda)} \quad (6)$$

is a special function, called the Melnikov–Arnold integral, as defined in [11]; expressions for $A_n(\lambda)$ at any natural n ($n = 1, 2, \dots$) and for kindred functions are given in [22].

One iteration of map (4) corresponds to one period of the model pendulum rotation, or a half-period of its libration. The motion of system (3) is mapped by Eqs. (4) asynchronously: the action-like variable w is taken at $\varphi = \pm\pi$, while the perturbation phase τ is taken at $\varphi = 0$. The desynchronization can be removed by a special procedure [22].

An equivalent form of map (4), as used, e. g., in [10, 30], is given by

$$\begin{aligned} y' &= y + \sin x, \\ x' &= x - \lambda \ln |y'| + c \pmod{2\pi}, \end{aligned} \quad (7)$$

where $y = \frac{w}{W}$, $x = \tau + \pi$; and

$$c = \lambda \ln \frac{32}{|W|} \quad (8)$$

is a new constant parameter. This form of the separatrix map is especially simple-looking; therefore, we call it the “form in natural variables.”

On various generalizations of the separatrix map theory (in particular, for cases of asymmetric perturbation and multiple interacting resonances) see [27, 30].

Linearizing the separatrix map (7) in y near a fixed point (near a resonant y value, and $\sin x$ is not linearized), one gets the standard map [11]:

$$\begin{aligned} y' &= y + K \sin x \pmod{2\pi}, \\ x' &= x + y' \pmod{2\pi}, \end{aligned} \quad (9)$$

where K is the so-called stochasticity parameter. It is related to λ and the resonant $y = y_{\text{res}}$ value by the formula $K = \lambda/y_{\text{res}}$ [11].

Note that y in Eqs. 9 is not the same variable as in Eqs. (7). In Eqs. 9, y is a rescaled energy around a given resonant value.

3 Lyapunov exponents and dynamical entropy

The Lyapunov characteristic exponents (LCEs) characterize the rate of divergence of trajectories close to each other in phase space; see, e. g., [18]. A nonzero LCE indicates chaotic character of motion, while the maximum LCE equal to zero is the signature of regular (periodic or quasi-periodic) motion. The Lyapunov time (the quantity reciprocal to the maximum LCE) characterizes predictability time of the motion: in fact, it provides a lower bound to the predictable dynamics, since the timescale for any macroscopical change in the orbit is given by the diffusion time $T_d \gg T_L$; see [12]. Therefore, calculation of LCEs is one of the most important instruments in nonlinear dynamics.

Let us consider two trajectories initially close to each other in phase space. One of them we shall refer to as the *guiding* trajectory and the other as the *shadow* one. Let $d(t_0)$ be the length of the displacement vector directed from the guiding trajectory to the shadow one at an initial moment $t = t_0$. The maximum LCE is defined by the formula [18]:

$$L = \limsup_{\substack{t \rightarrow \infty \\ d(t_0) \rightarrow 0}} \frac{1}{t - t_0} \ln \frac{d(t)}{d(t_0)}. \quad (10)$$

Our numerical data concern the maximum Lyapunov exponent L of the motion in the chaotic layer in the separatrix map's phase space, the layer's measure μ_{ch} , and the product of L and μ_{ch} . All these data were obtained by means of numerical experiments with map (7).

The initial data were taken inside the chaotic layer. The Lyapunov exponents were computed by the tangent map method (described, e. g., in [11]).

In parallel with the maximum Lyapunov exponent L for each trajectory, the corresponding value of the chaotic layer half-width $y_b(\lambda)$ was computed, as attained by the same trajectory. The chaotic layer half-width y_b corresponds to the maximum deviation of $|y_i|$ (from the unperturbed separatrix) of any trajectory inside the chaotic layer. It can be obtained as the $|y_i|$ maximum achieved by a single chaotic trajectory, if the number of iterations of

the map is large enough. The λ dependence for y_b is therefore constructed as follows [29]. At each step in λ , the value of c corresponding to the minimum y_b is found (over the $0 \leq c < 2\pi$ interval, by varying the c value with a small step) and the minimum y_b is plotted against the current λ value. The obtained y_b value corresponds to the case of the least perturbed border, because, by the given procedure, the contribution of marginal resonances is minimized.

The number $n_{\text{it}} = 10^7$ of iterations was found to be sufficient to saturate the values of both L and y_b , as verified by comparing the results with those obtained using the computation time ten times less, i. e., with $n_{\text{it}} = 10^6$.

To take into account the “quasi-sinusoidal” form of the last invariant curve that serves as the chaotic layer’s border, the layer half-width value y_b was calculated as the average of the maximum and minimum values of $|y|$ at the border, attained during each computation.

The numerical data cover the interval in λ from zero up to 5. This interval is sufficient for our study, because at greater values of λ the asymptotic behaviours of L and μ are in principle well established; see [23, 30] and a discussion below. The resolution (step) in $\lambda \in [0, 5]$ was set equal to 0.01. At each step in λ , the values of L were computed for 40 values of c equally spaced in the interval $[0, 2\pi]$, and the value of c corresponding to the minimum width of the layer (the case of the least perturbed border) was fixed. The corresponding values of L and y_b , as functions of the adiabaticity parameter λ , were plotted.

Note that the case of the least perturbed border is generic in applications, because the border perturbations are strong only locally in c ; for details see [30].

In Fig. 1 (left panel), we present the obtained λ dependences for the maximum Lyapunov exponent L (red dots) and the chaotic layer half-width y_b (blue dots). The both dependences do not look quite simple; however, a rational function fitting is suitable for $L(\lambda)$ [23, 30], and a piecewise-linear fitting for $y_b(\lambda)$; see [30, fig. 5.6]. In asymptotic regimes $\lambda \ll 1$ and $\lambda \gg 1$, these dependences allow for theoretical interpretations; see reviews on them in [30]. On the structure and width parameters of the chaotic layer see also [9, 33].

In Fig. 1 (right panel), the λ dependence of the product $L(\lambda) \cdot y_b(\lambda)$ is shown (green dots). The data for L and y_b presented in the left panel of Fig. 1 were used to construct it.

Taking into account that x is defined on the segment $[0, 2\pi]$ and y_b rep-

resents the chaotic layer's half-width, the phase space chaotic component's measure is given by the formula

$$\mu_{\text{ch}}(\lambda) = 4\pi\sigma(\lambda)y_{\text{b}}(\lambda). \quad (11)$$

Here the coefficient σ is the ratio of the area of the chaotic component inside the chaotic layer to the layer's total area (as bounded by the layer's external borders); thus, this coefficient accounts for the layer's "porosity" [25]. The quantity $1 - \sigma$ is nothing but the total relative area of all regular islands inside the layer.

In the limit $\lambda \gg 1$ and in the least perturbed border case, the porosity was calculated in [25] using the formula

$$\sigma = \lim_{\lambda \rightarrow \infty} y_{\text{b}}^{-1} \int_0^{y_{\text{b}}} \tilde{\mu}_{\text{ch}}(y) dy = K_{\text{G}} \int_{K_{\text{G}}}^{\infty} \mu_{\text{st}}(K) \frac{dK}{K^2}, \quad (12)$$

where $\tilde{\mu}_{\text{ch}}(y)$ is the local relative measure of the chaotic component of the separatrix map phase space, and $\mu_{\text{st}}(K)$ is the relative measure of the chaotic component of phase space of the standard map (9). The quantity K_{G} is the critical value of the stochasticity parameter K [20]: $K_{\text{G}} = 0.971635406\dots$

According to [25], in the limit $\lambda \rightarrow \infty$ one has $\sigma \approx 0.780$, and, in the function

$$h(\lambda) = C_1\lambda,$$

the coefficient

$$C_1 = C_{\text{h}}\sigma \approx 0.625,$$

where $C_{\text{h}} \approx 0.801$ is Chirikov's constant (the maximum Lyapunov exponent of the separatrix map in the limit $\lambda \rightarrow \infty$, see [25]).

The green dots in the right panel of Fig. 1 represent the multiplication of the two curves in the left panel. Although the slope for $y_{\text{b}}(\lambda)$ at $\lambda > 1/2$ (left panel, blue dots) seems to be close to strictly 1, a closer inspection of the graph shows that, at λ near $1/2$, the slope deviates from unity quite essentially. The visible restricted deviations of the dynamical entropy (right panel, green dots), as a function of λ , from the linear law might be due to numerical indefiniteness of the layer porosity, which should be taken into

account when calculating the chaotic domain measure, but which is indeed hard to evaluate.

In Fig. 1 (right panel), the violet straight line hypothetically describes the expected dependence $h(\lambda)$, on taking into account the chaotic layer porosity σ (in the limit $\lambda \gg 1$, where $\sigma \approx 0.78$). Upon this improvement, the over-all slope of the dependence obviously looks much more close to $1/2$ (the initial slope observed at $\lambda \lesssim 1/2$).

Form (7) of the separatrix map is that in natural variables (x, y) , as defined above. We see that, adopting this form, one has

$$h \approx 2\pi\lambda, \quad (13)$$

because the layer's span in x is 2π .

Returning to the separatrix map form (4), i. e., the form in original variables (τ, w) , in which the layer half-width $w_b = Wy_b$, and W is given by formula (5), one finds the dynamical entropy

$$h \approx 2\pi\lambda W = 8\pi^2\varepsilon \frac{\lambda^3}{\sinh \frac{\pi\lambda}{2}} \quad (14)$$

over the whole range $\lambda \in [0, \infty]$. Note that $h(\lambda)$ turns out to be expressed through the ‘‘Bose–Einstein function’’ $1/\sinh(\alpha\lambda)$, where α is constant.

If, in the initial Hamiltonian (3) one sets $k = 1/2$ instead of $k = 1$, keeping $a = b$, then, according to [22, eqs. (12) and (A.12)],

$$W = \varepsilon\lambda(A_1(\lambda) + A_1(-\lambda)) = \frac{2\pi\varepsilon\lambda}{\cosh \frac{\pi\lambda}{2}}, \quad (15)$$

where $\varepsilon = a/\mathcal{F}$, as defined above. Therefore, for the separatrix map in original variables (τ, w) one gets the dynamical entropy in the form

$$h \approx 2\pi\lambda W = 4\pi^2\varepsilon \frac{\lambda^2}{\cosh \frac{\pi\lambda}{2}}, \quad (16)$$

again over the whole range $\lambda \in [0, \infty]$. Note that here $h(\lambda)$ is expressed through the ‘‘Fermi–Dirac function’’ $1/\cosh(\alpha\lambda)$.

The examples, given by Eqs. (14) and (16), demonstrate that the intrinsic quasilinear (or perhaps exactly linear) relationship λ – h for the separatrix map in natural variables forms a basis for calculating the dynamical entropy for any perturbed nonlinear resonance, in its first fundamental model, if Melnikov–Arnold integrals are known.

4 Discussion

The adiabaticity parameter λ , which is the ratio of the perturbation frequency Ω to the frequency ω_0 of small-amplitude oscillations on resonance, is the main parameter of the problem. It characterizes the separation of the perturbing and guiding resonances in units of one quarter of the guiding resonance width. Indeed, $\lambda = \Omega/\omega_0$, and the separation of resonances in frequency space is equal to Ω , whereas the guiding resonance width is equal to $4\omega_0$ [11]. If, in the Hamiltonian system (3), the perturbation frequency is relatively large, the separation of resonances in the canonical momentum is also large and they almost do not interact. On reducing the frequency of perturbation, they approach each other, and appreciable chaotic layers emerge in the vicinity of the separatrices. On reducing the frequency of perturbation further on, the layers merge into a single chaotic layer, due to the strong resonance overlap. Therefore, the adiabaticity parameter λ can be regarded as a kind of a resonance-overlap parameter. In the asymptotic limit of the adiabatic perturbation, $\lambda \ll 1$, the resonances in the multiplet strongly overlap, while in the asymptotic limit of the non-adiabatic perturbation, $\lambda \gg 1$, the resonances are separated and do not interact.

Up to here we have considered the motion inside the main chaotic layer of the separatrix map, ignoring the smaller chaotic layers not connected heteroclinically with the main layer; these layers are present around the resonances external to the main layer. How large can be the contribution of these external chaotic domains to the total dynamical entropy of the separatrix map, i.e., the dynamical entropy calculated over the whole phase space of the map? It turns out to be rather small, as we find in the following.

According to [25, eq. 10], at $\lambda \gg 1$, the dynamical entropy inside the main chaotic layer can be represented as

$$h(\lambda) = C_1 \lambda, \quad (17)$$

with

$$C_1 = K_G \int_{K_G}^{\infty} h_{\text{standard}}(K) \frac{dK}{K^2} \approx 0.625. \quad (18)$$

Here $h_{\text{standard}}(K)$ is the dynamical entropy of the standard map as a function of the stochasticity parameter K .

For the dynamical entropy *outside* the main layer, one analogously arrives at

$$h_{\text{aux}}(\lambda) = C_2\lambda, \quad (19)$$

where

$$C_2 = K_G \int_0^{K_G} h_{\text{standard}}(K) \frac{dK}{K^2}. \quad (20)$$

A theoretical approximation for the dynamical entropy $h_{\text{standard}}(K)$ of the standard map at $K \in [0, 1]$ is given by the function [24]:

$$h_{\text{standard}}(K) = AK^{1/2} \exp\left(-\frac{\pi^2}{K^{1/2}}\right) \quad (21)$$

with $A = 929.6 \pm 4.0$. Then, one obtains

$$C_2 = AK_G \int_0^{K_G} \exp\left(-\frac{\pi^2}{K^{1/2}}\right) \frac{dK}{K^{3/2}} = \frac{2AK_G}{\pi^2} \exp(x) \Big|_{x=-\infty}^{x=\pi^2/\sqrt{K_G}} \approx 0.00820. \quad (22)$$

The contribution of the external chaotic component to the total dynamical entropy of the separatrix map is thus relatively small, because $C_2 < 0.01$. Indeed, in the given limit of large $\lambda \gg 1$, the calculated total dynamical entropy $h_{\text{total}} = C_1\lambda + C_2\lambda \approx 0.633\lambda$ is almost the same as the dynamical entropy $h = C_1\lambda \approx 0.625\lambda$ calculated for the motion in the main chaotic layer.

Let us briefly discuss the role of the parameter c . By considering the dynamical entropy instead of the Lyapunov exponents and the chaotic domain measure, the sharp local variations of the latter two quantities, prominent in their dependences on λ , are also expected to be smoothed out when one considers dependences on the parameter c . This is illustrated in Fig. 2, where we present computed dependences of the λ -normalized maximum Lyapunov exponent L and the chaotic domain measure μ on the parameter c at a fixed value of λ ($\lambda = 0.01$). The measure μ was computed here following an approach adopted in [11, 24, 28]; it takes into account the variation of the chaotic layer porosity (the presence of regular islands inside the layer) with c . Namely, to compute μ , the traditional ‘‘one trajectory method’’ was used: the number of cells, explored by a single trajectory on a grid exposed over the chaotic domain, was calculated. The grid was set to consist of 2000×2000 pixels. At each step in c , the map (7) was iterated 10^8 times, sufficient to saturate the computed values of μ and L . The step in c was set to 0.001.

From the graphs in Fig. 2, it is obvious that the variations in L and μ are anticorrelated, and, therefore, the multiplication of the two curves, which gives the dynamical entropy, provides a significantly smoothed curve. This again underlines that the dynamical entropy is a much more fundamental property, as compared to L and μ . This example demonstrates that the λ -normalized dynamical entropy h might stay constant (at least approximately) not only with variation of λ , but also with variation of c .

The numerical methods used above require quite a lot of computing time to achieve reliable results. In this respect, it is worth noting that both the maximum Lyapunov exponent and the chaotic layer width may also be conveniently computed by applying techniques of the dynamical exponent curves [16, 15], which have straightforward interpretations for these computable quantities, and may require fewer data points than used above. In future, efforts can be made to connect further relevant studies with the exponent curves.

Concerning further applications of the results presented in this article, one should outline that, if the constancy of the λ -normalized dynamical entropy were verified analytically, this constancy would provide a convenient framework to evaluate the measure μ of chaotic domains in phase space in various physical models (mentioned already above), as soon as the maximum Lyapunov exponent is calculated. This is important because any calculations of μ are much more complicated and computationally expensive than those of L .

As already mentioned in the Introduction, the employed model relates with particularly interesting physical phenomena and is both applicable to a broad spectrum of physical phenomena. It should also be noted that the given study subject can be expanded, to encompass the separatrix map generalizations. The generalized separatrix maps are characterized by the τ increments (in equations (4)) that are algebraic (power-law with various power-law indices), not logarithmic ones; see [30] for examples. A particular generalized map is used to describe dynamical environments of cometary nuclei [17].

5 Conclusions

In this article, we have calculated the maximum Lyapunov exponent of the motion in the separatrix map's chaotic layer, along with calculation of its width, as functions of the adiabaticity parameter λ . The case of the layer's

least perturbed border has been considered.

However, although these obtained dependences are not at all simple-looking, the dynamical entropy h of the separatrix map (in natural variables) has turned out to be an almost-linear function of λ ; in other words, if normalized by λ , the entropy is a quasi-constant.

Thus, the formula for dynamical entropy of the separatrix map (7) has turned out to be rather simple (quasilinear in λ), in contrast to the much more complicated behavior of the maximum Lyapunov exponent and the layer width. This is no wonder, since the dynamical entropy is a more fundamental property of the motion than the latter two.

To calculate the dynamical entropy more precisely, the layer's porosity σ must be taken into account as a function of λ ; this represents a perspective numerical-experimental and/or theoretical problem. As demonstrated in our study, even an approximate accounting for σ makes the observed numerical-experimental dependence $h(\lambda)$ much closer to a linear one.

The intrinsic quasilinear (or perhaps exactly linear) relationship λ - h for the separatrix map in natural variables forms a basis for calculating the dynamical entropy for any perturbed nonlinear resonance in the first fundamental model, as soon as the corresponding Melnikov–Arnold integral is known.

Acknowledgements

The author is most thankful to Pablo Cincotta for invaluable comments. The author would like to thank the referees for remarks and comments which greatly improved the manuscript.

The author declares no conflict of interest.

References

- [1] S. S. Abdullaev. *Construction of Mappings for Hamiltonian Systems and Their Applications*. Springer, Berlin Heidelberg, 2006.
- [2] S. S. Abdullaev. *Magnetic Stochasticity in Magnetically Confined Fusion Plasmas*. Springer International Publishing, Switzerland, 2014.

- [3] S. S. Abdullaev and G. M. Zaslavsky. Self-similarity of stochastic magnetic field lines near the X-point. *Physics of Plasmas*, 2(12):4533–4541, December 1995.
- [4] S. S. Abdullaev and G. M. Zaslavsky. Application of the separatrix map to study perturbed magnetic field lines near the separatrix. *Physics of Plasmas*, 3(2):516–528, February 1996.
- [5] Taehoon Ahn, Gwangil Kim, and Seunghwan Kim. Analysis of the separatrix map in Hamiltonian systems. *Physica D Nonlinear Phenomena*, 89(3):315–328, January 1996.
- [6] G. Benettin, L. Galgani, and J. M. Strelcyn. Kolmogorov entropy and numerical experiments. *Phys. Rev. A*, 14(6):2338–2345, December 1976.
- [7] Alessandra Celletti. Analysis of resonances in the spin-orbit problem in Celestial Mechanics: The synchronous resonance (Part I). *Zeitschrift Angewandte Mathematik und Physik*, 41(2):174–204, March 1990.
- [8] B. V. Chirikov. Research concerning the theory of nonlinear resonance and stochasticity. *CERN Trans.*, 71–40:1–118, October 1971.
- [9] B. V. Chirikov and D. L. Shepelyansky. Statistics of Poincaré recurrences and the structure of the stochastic layer of the nonlinear resonance. *INP Preprint*, 81–69:1–16, 1981.
- [10] B. V. Chirikov and D. L. Shepelyansky. Correlation properties of dynamical chaos in Hamiltonian systems. *Physica D Nonlinear Phenomena*, 13(3):395–400, November 1984.
- [11] Boris V. Chirikov. A universal instability of many-dimensional oscillator systems. *Phys. Rep.*, 52(5):263–379, May 1979.
- [12] Pablo M. Cincotta, Claudia M. Giordano, and Ivan I. Shevchenko. Revisiting the relation between the Lyapunov time and the instability time. *Physica D Nonlinear Phenomena*, 430:133101, February 2022.
- [13] D. F. Escande. Stochasticity in classical Hamiltonian systems: Universal aspects. *Phys. Rep.*, 121(3-4):165–261, May 1985.

- [14] D. F. Escande and F. Doveil. Renormalization method for computing the threshold of the large-scale stochastic instability in two degrees of freedom Hamiltonian systems. *Journal of Statistical Physics*, 26(2):257–284, October 1981.
- [15] J. B. Gao, J. Hu, W. W. Tung, and Y. H. Cao. Distinguishing chaos from noise by scale-dependent Lyapunov exponent. *Phys. Rev. E*, 74(6):066204, December 2006.
- [16] J. B. Gao, S. K. Hwang, and J. M. Liu. When can noise induce chaos? *Phys. Rev. Lett.*, 82(6):1132–1135, February 1999.
- [17] José Lages, Ivan I. Shevchenko, and Guillaume Rollin. Chaotic dynamics around cometary nuclei. *Icarus*, 307:391–399, June 2018.
- [18] A. J. Lichtenberg and M. A. Leiberman. *Regular and Chaotic Dynamics*. Springer, New York, 1992.
- [19] Renu Malhotra. Capture probabilities for secondary resonances. *Icarus*, 87(2):249–264, October 1990.
- [20] J. D. Meiss. Symplectic maps, variational principles, and transport. *Reviews of Modern Physics*, 64(3):795–848, July 1992.
- [21] Alice C. Quillen and Abobakar Sediq Miakhel. Quantum chaos on the separatrix of the periodically perturbed Harper model. *arXiv e-prints*, December 2024.
- [22] I. I. Shevchenko. Geometry of a chaotic layer. *Journal of Experimental and Theoretical Physics*, 91(3):615–625, September 2000.
- [23] I. I. Shevchenko. Maximum Lyapunov exponents for chaotic rotation of natural planetary satellites. *Cosmic Research*, 40(3):296–304, May 2002.
- [24] I. I. Shevchenko. Isentropic perturbations of a chaotic domain. *Physics Letters A*, 333(5-6):408–414, December 2004.
- [25] I. I. Shevchenko. On the maximum Lyapunov exponent of the motion in a chaotic layer. *Journal of Experimental and Theoretical Physics Letters*, 79(11):523–528, June 2004.

- [26] I. I. Shevchenko. Lyapunov exponents in fundamental models of nonlinear resonance. *Journal of Experimental and Theoretical Physics Letters*, 120(8):622–629, 2024.
- [27] Ivan I. Shevchenko. The separatrix algorithmic map: Application to the spin-orbit motion. *Celestial Mechanics and Dynamical Astronomy*, 73:259–268, January 1999.
- [28] Ivan I. Shevchenko. Adiabatic chaos in the Prometheus–Pandora system. *MNRAS*, 384(3):1211–1220, March 2008.
- [29] Ivan I. Shevchenko. The width of a chaotic layer. *Physics Letters A*, 372(6):808–816, February 2008.
- [30] Ivan I. Shevchenko. *Dynamical Chaos in Planetary Systems*. Springer Nature, Cham, 2020.
- [31] V. V. Vecheslavov. Motion in the vicinity of the separatrix of a nonlinear resonance in the presence of high-frequency excitations. *Journal of Experimental and Theoretical Physics*, 82(6):1190–1195, June 1996.
- [32] V. V. Vecheslavov. Fine structure of splitting of the separatrix of a nonlinear resonance. *Journal of Experimental and Theoretical Physics*, 89(1):182–187, July 1999.
- [33] V. V. Vecheslavov. Chaotic layer of a pendulum under low-and medium-frequency perturbations. *Journal of Technical Physics*, 49(5):521–525, May 2004.
- [34] J. Wisdom, S. J. Peale, and F. Mignard. The chaotic rotation of Hyperion. *Icarus*, 58(2):137–152, May 1984.
- [35] G. M. Zaslavsky and S. S. Abdullaev. Scaling properties and anomalous transport of particles inside the stochastic layer. *Phys. Rev. E*, 51(5):3901–3910, May 1995.

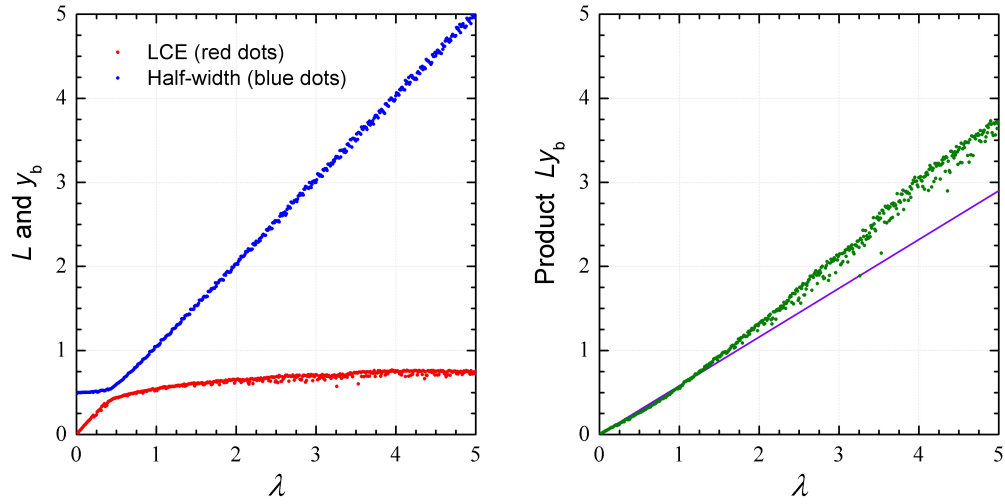


Figure 1: Left panel: The dependences of the maximum Lyapunov exponent L (red dots) and the chaotic layer half-width y_b (blue dots) on the adiabaticity parameter λ , as obtained in our numerical experiments. Right panel: The λ dependence of the dynamical entropy $h = L \cdot y_b$ (green dots). The violet straight line represents an expected function $h(\lambda)$, when the porosity of the chaotic layer is approximately taken into account, as explained in the text.

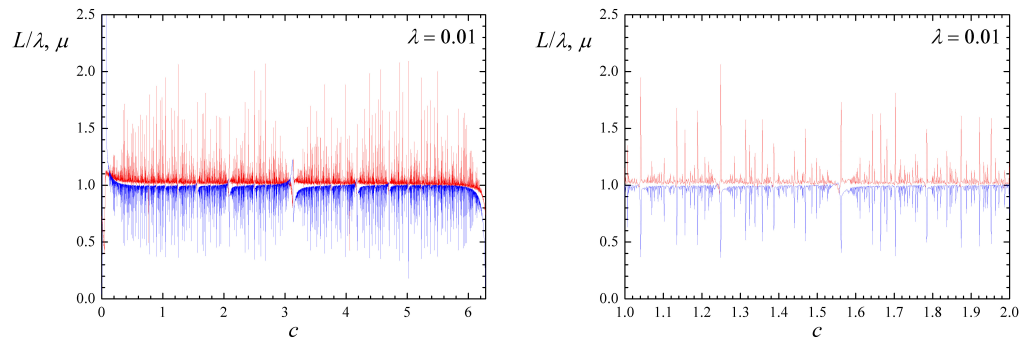


Figure 2: Left panel: The parameter c dependences of L/λ (the λ -normalized maximum Lyapunov exponent L ; red dots) and the chaotic domain measure μ (blue dots), at a fixed value of λ (set equal to 0.01). Right panel: the graph's detail given in a higher resolution.